ELSEVIER

Catalysis Today 71 (2001) 161–167

CATALYSIS TODAY

www.elsevier.com/locate/cattod

Insertion of iron-complex to lamellar vanadyl benzylphosphate for preparation of well-defined catalyst

Atsushi Satsuma [a,*], Yuki Kijima [a], Shin-ichi Komai [a], Yuichi Kamiya [b], Eiichiro Nishikawa [b], Tadashi Hatttori [a]

[a] *Department of Applied Chemistry, Graduate School of Engineering, Nagoya University, Furo-cho, Chikusa-ku, Nagoya 464-8603, Japan*
[b] *Japan Chemical Industry Association, Kasumigaseki 3-2-6, Chiyoda-ku, Tokyo 100-0013, Japan*

Abstract

A novel approach for preparation of promoted vanadium-phosphorous oxide (VPO) in well-defined structure was examined. Lamellar vanadyl benzylphosphate (LVPO) was used as a host material and Fe-complex as a guest. It was found that Fe-complex was successfully inserted into LVPO by heating of LVPO and $Fe(acac)_3$ in toluene solution. The obtained material was characterized by means of XRD, TEM, EDX, XPS, and FT/IR. It was confirmed that $Fe(acac)_3$ was uniformly dispersed in the interlayer of LVPO without significant distraction of lamellar structure of parent LVPO.

Keywords: Preparation; Vanadium-phosphorous oxide; Lamella compound; Intercalation

1. Introduction

1.1. $(VO)_2P_2O_7$ for n-butane oxidation and effect of promoters

Vanadyl pyrophosphate, $(VO)_2P_2O_7$, has been widely accepted as an active and selective phase for partial oxidation of *n*-butane to maleic anhydride [1–7]. For improvement in catalytic performance, industrial $(VO)_2P_2O_7$ catalysts contain additional cations those act as promoters of different kind. Various types of elements, such as Co, Mo, Cr, Fe, Ce, Zn, Ti, Zr, Si and so on, can be found in patents, and some of scientific literature clarified the effect of those promoters.

Haber and coworkers [8] clarified that the incorporation of Li, Na, K, Cs, Be, Mg, Ca, and Ba can easily donate electrons to the framework of vanadyl phosphate, leading to an increase in the negative charge of oxygen atom and in the rate of butane oxidation. They concluded that the high activity in butane oxidation and high selectivity to MA requires a fine tuning of the basicity of surface oxygen atoms to accelerate the activation of butane and of the acidity of surface to secure the appropriate time of the reaction intermediates. Takita et al. [9] observed a linear relationship between catalytic activity for MA formation and the frequency of the V=O vibration of solids containing different promoters (Mn, Co, Fe, Zn, and Zr).

On the other hand, promoters can optimize preparation conditions and structures of $(VO)_2P_2O_7$. As reported by Horowitz et al. [10], the addition of tetraethyl orthosilicate is thought to eliminate water as a by-product in the organic solvent, leading to the formation of $(VO)_2P_2O_7$ having favorable morphology.

* Corresponding author. Tel.: +81-52-789-4608; fax: +81-52-789-3193.
E-mail address: satsuma@apchem.nagoya-u.ac.jp (A. Satsuma).

0920-5861/01/$ – see front matter
PII: S0920-5861(01)00426-6

The structural modification of $(VO)_2P_2O_7$ is also regarded as an important effect of promoters. The structural disorder, which is related to the broadening of the (2 0 0) line in XRD patterns, is related to high activity of VPO prepared from organic media [11–14]. In the case of promoted $(VO)_2P_2O_7$, Ye et al. [13] reported that the activity per surface V=O species was found to be dependent on the disorder of VPO crystal along the (1 0 0) plane, which can be controlled by the addition of various promoters.

These various roles of promoters have been categorized. Hutchings [4] classified into two types of promoters which (1) enable the formation of the required V–P phase, and (2) form solid solutions with the active phase which regulate the catalytic activity. Cavani and Trifiro [6] summarized that the additives can be divided into following three groups: (1) ions (Zn and Co) that interact with free phosphoric acid acting as a tool of fine tuning of the optimal surface P/V ratio and acidity, (2) ions (S and Si) that can substitute for phosphorous in the precursor controlling the morphology and defects of $(VO)_2P_2O_7$ after calcination, and (3) transition metal ions (e.g., Ti, Zr, Ce, and Mo) that substitute for vanadium acting as real modifiers directly involved in the reaction pattern. Latter two types of promoters directly interact to $(VO)_2P_2O_7$, i.e., (1) modification of structural features of $(VO)_2P_2O_7$, (2) modification of chemical properties of $(VO)_2P_2O_7$, e.g., acidity, basicity, and V=O species as redox sites.

Since preparation method for addition of promoters often strongly affects on these features of promoted VPO catalysts, a novel preparation method would result in fine control of promoted VPO structures and be a possible break-through for the enhancement of catalytic performance. Intercalation is one of the candidates for the preparation of tailored VPO catalysts, as Datta and Keller [15] demonstrated incorporation of $Pd(NO_3)_2$ into $VOHPO_4{\cdot}0.5H_2O$. Although VPO catalysts are usually prepared from $VOHPO_4{\cdot}0.5H_2O$ as a precursor, use of other material having wide range of flexibility may result in the fine-control of the structure and chemical properties.

1.2. $(VO)_2P_2O_7$ and related VPO compounds

It has been paid much attention on a series of vanadium phosphate (VPO) chemistry, because of wide structural diversity and high dependence of catalytic performance on the crystal phase. Currently, VPO compounds having novel structures have been synthesized by means of intercalation of various organic compounds [16–25]. Benzinger and coworkers [19,21] demonstrated an intercalation of *n*-alkylamines into $VOHPO_4{\cdot}0.5H_2O$. Formation of ordered lamellar structure of VPO compound incorporating *n*-tetradecyltrimethyl ammonium into $VOHPO_4{\cdot}0.5H_2O$ was clearly shown by Miyake and coworkers [22]. Okuhara and coworkers [24,25] successfully demonstrated "exfoliation", which is intercalation of 4-butylaniline into $VOPO_4{\cdot}2H_2O$ followed by stirring in THF, and deposition of thin lamella onto alumina support.

A series of VPO compounds with lamellar structure is the most interesting materials. Vanadyl alkylphosphonates [17,18,20,23] having the formula of $VO(RO)_x(HO)_{1-x}PO_3 \cdot (ROH)_y(H_2O)_z$ has a lamella structure with alternating inorganic and organic layers, and the intercalation property of vanadyl alkylphosphonate was greatly dependent on shape and size of the alkyl group [26]. On the other hand, DuPont's researchers recently claimed that vanadyl alkylphosphate which has P–O–C bond with a lamellar structure could be synthesized through reacting V_2O_5 with P_2O_5 in alcohol [27]. Although this method is applicable only for intercalation of primary aliphatic alcohol, Kamiya et al. [28,29] developed a different method that enables to intercalate not only primary alcohol but also secondary aliphatic and alicyclic alcohols. This method can control the distance of interlayer in the range from 0.91 to 2.37 nm, and the distance linearly increases with molecular diameter of alcohols, indicating ordered filling of the interlayer with alcohols. It can be expected that the use of these LVPO materials as precursors may open up a novel method for fine control of promoted VPO catalysts.

1.3. Possible method for preparation of well-defined VPO

Use of lamellar compounds as precursors for VPO catalysts would be very useful because of high potential of interlayer nano-space for catalyst design. Since the interlayer of VPO compounds is acidic, intercalation of basic amine molecules may too much stabilize the lamella structure, and thus further modification is

expected to be difficult. The lamellar VPO-containing alcohols is expected to be more suitable for further modification because of weaker bonding of VPO layers. After insertion of metal-complexes followed by calcination, promoter ions can be uniformly fixed in the interlayer. This nano-structural modification of VPO may results in fine-control of oxidation activity or acid–base property. Furthermore, the heteroatoms in the interlayer may cause some disorder of VPO crystal, which often play an important role in the enhancement of catalytic performance.

In the present study, we demonstrate a potential method for preparation of well-defined promoted VPO catalysts. Lamellar vanadyl benzylphosphate (LVPO) incorporating benzyl alcohol was used as a host, because of sufficient distance of interlayer space (ca. 1.8 nm) for various metal-complexes. The possible advantage of this material is hydrophobic property of the interlayer, which makes a favorable field for coordination compounds. This report focuses on insertion of Fe-complexes into the interlayer of LVPO. The obtained materials are characterized to confirm the layered structure and dispersion of metal compounds.

2. Experimental

2.1. Preparation of catalysts

LVPO was prepared by the method reported elsewhere [28,29]. V_2O_5 (29.2 g, Kishida, 99%) was reduced in mixture of *iso*-butyl alcohol (180 cm^3, Kishida, 99.5%) and benzyl alcohol (120 cm^3, Kishida, 99.5%) at refluxing temperature for 3 h. The resulted black solid was separated by filtration and confirmed to be a mixture of V_2O_5 and V_4O_9 by XRD. The solid was suspended in 300 cm^3 of benzyl alcohol, then a suspension of P_2O_5 in 75 cm^3 of toluene was slowly added with stirring. Then the mixture was refluxed for 6 h until valence of vanadium in obtained VPO reached +4. After cooling to room temperature, the obtained blue solid was filtered and washed with 250 cm^3 of acetone, and then dried at room temperature in air for 12 h.

For the insertion of Fe-complex, benzyl alcohol or toluene (Kishida, 99.5%) was used as a solvent, and $Fe(acac)_3$ (Kishida, 98%) and ferrocene (Kishida, 98%) were used as a guest molecule. LVPO and Fe-compound at a loading ratio of $Fe/V = 0.5$ were dissolved in 36 cm^3 of the solution and heated at 358 K with stirring for 3 h. The obtained solid was filtered, washed with 40 cm^3 of acetone, and then dried at room temperature in air for 12 h. The preparation conditions of the samples were summarized in Table 1.

2.2. Characterizations

XRD patterns were recorded with Rigaku RINT-1200 diffractometer using Cu Kα as a target. XPS spectra were measured with Shimazu ESCA-3300 using Mg Kα as a target. SEM images were taken by HITACHI S-800S. TEM and EDS images were taken by JEOL JEM-2010 coupled with Voyager III EDS analyzer, respectively. Chemical compositions of obtained materials were measured by Jarrell-Ash 975 PLASMA ATOMCOMP inductive coupled plasma spectrometer. Elemental analysis was performed by Microanalytisch Labor Pascher, Germany.

3. Results and discussion

3.1. Preparation conditions

Fig. 1 shows XRD patterns of LVPO and these after the insertion of Fe-complexes. Before insertion

Table 1
Preparation conditions, chemical compositions, and $d(0\,0\,1)$ in parent LVPO and Fe-loaded LVPO

Sample	Prepration		Atom ratio in bulk					Fe/V in surface	$d(0\,0\,1)$ (nm)
	Solvent	Fe source	P/V	C/V	O/V	H/V	Fe/V		
LVPO	–	–	0.94	8.56	5.44	10.4	<0.001	<0.01	1.78
LVPO-Fe-A	Toluene	$Fe(acac)_3$	1.01	5.71	5.69	7.19	0.084	0.18	1.46
LVPO-Fe-B	Toluene	Ferrocene	0.99	5.34	5.46	6.73	0.023	0.09	1.33
LVPO-Fe-C	Benzyl alcohol	$Fe(acac)_3$	1.02	5.20	5.53	6.69	0.020	0.09	1.33
LVPO-Fe-D	Benzyl alcohol	Ferrocene	0.98	8.40	5.74	9.77	0.007	0.08	1.74

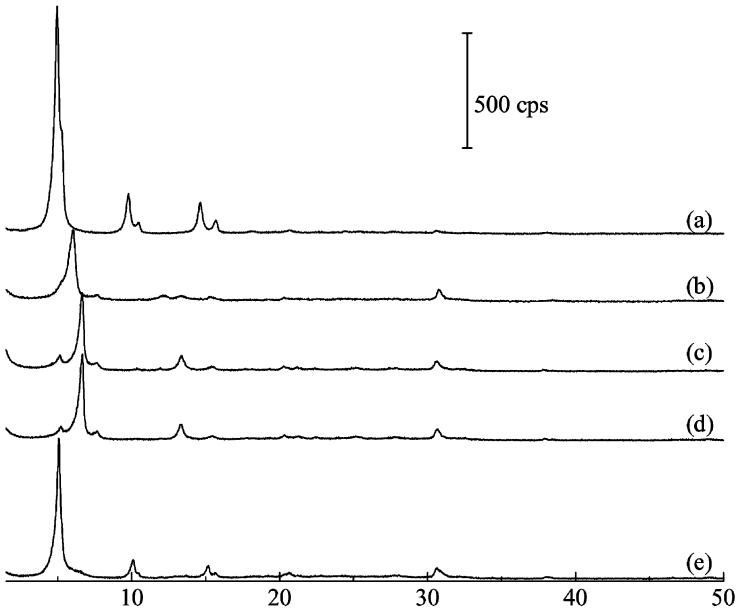

Fig. 1. XRD patterns of: (a) parent LVPO, (b) LVPO-Fe-A, (c) LVPO-Fe-B, (d) LVPO-Fe-C and (e) LVPO-Fe-D.

of Fe-complexes, the XRD pattern exhibited strong diffraction line attributable to the (0 0 1) at $2\theta = 4.95^\circ$ with a shoulder at 5.28°. Weak diffraction lines were also observed at 9.76° and 14.6°, which can be attributable to the (0 0 2) and the (0 0 3), representing lamellar structure of LVPO having the d(0 0 1) value of 1.78 nm [28]. Weak lines were also observed at 10.4 and 15.7, representing contaminant lamella phase having the d(0 0 1) value of 1.67 nm. In the previous report, Kamiya et al. [29] showed a linear correlation between the d(0 0 1) value and molecular length of alcohol which corresponds to the distance between OH and farthest H. Molecular length of benzyl alcohol (0.709 nm) and the d(0 0 1) values (1.78 nm) also agree well with this correlation. Thus, benzyl alcohol should be present as a double layer tilting 56.6° against inorganic layer. A series of diffraction lines having the d(0 0 1) value of 1.67 nm indicates a minor phase. Since the molecular diameter of toluene (0.592 nm), which was used as a diluent of P_2O_5, is smaller than benzyl alcohol (0.709 nm), the minor phase could be LVPO phase incorporating toluene in the interlayer. After the insertion of Fe-complexes, the diffraction patterns of all the samples showed lamella structure, while decrease in the interlayer distance was observed. The presence of minor lamellar phase was not significant. The d(0 0 1) values of each samples were listed in Table 1.

Table 1 shows the Fe/V ratio of Fe-loaded LVPO. A part (17–1.4%) of Fe-complex was loaded in LVPO, though the Fe content was dependent on the preparation conditions in the sequence of A > B > C > D. The best condition for Fe-insertion was the use of $Fe(acac)_3$ as iron source and toluene as solvent. In the case of LVPO-Fe-A, the surface Fe/V ratio was only around twice as in the bulk, suggesting most of $Fe(acac)_3$ was inserted into LVPO bulk. The surface Fe/V ratio of other samples was 4–11 times higher than that in the bulk, suggesting higher concentration of Fe in the surface.

As a consequence, it was found that the insertion of Fe-complexes into LVPO is possible without significant destruction of LVPO structure. The use of toluene and $Fe(acac)_3$ was suggested to be the most suitable condition. In the next section, structure and Fe distribution of LVPO-Fe-A catalyst are characterized in detail.

3.2. Characterization of Fe-inserted LVPO

Fig. 2a shows SEM image of LVPO-Fe-A. The particles of LVPO-Fe-A were composed of plate-like

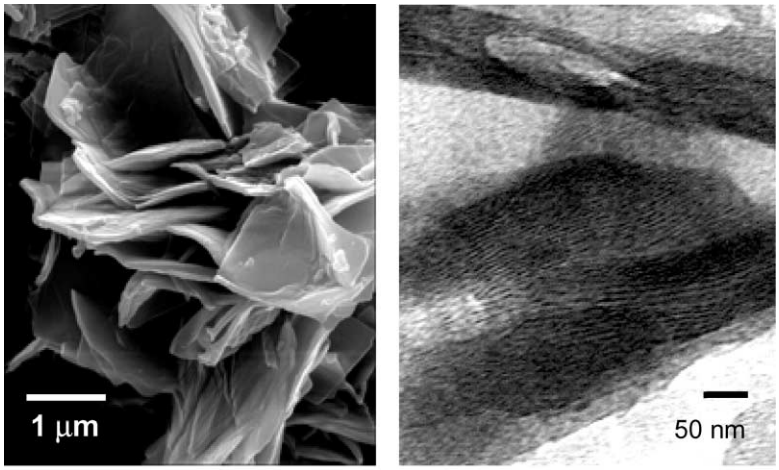

Fig. 2. SEM image (a) and TEM image (b) of LVPO-Fe-A.

crystallites. The size of crystallite was 1–3 μm in diameter and 50–100 nm in thickness. SEM images of parent LVPO and other Fe-loaded LVPO were almost the same in the shape of crystallites. Fig. 2b shows TEM image of the side view of crystallites. The TEM image clearly indicates the lamellar structure of LVPO-Fe-A. From the patterns of lamella, the interlayer distance can be estimated as ca. 1.5 nm, which agrees well with the estimation from XRD patterns.

Fig. 3 shows TEM image of LVPO-Fe-A and EDX images of V, P and Fe. The white points in the EDX images, which indicate the presence of the atoms, are agreed well with each other and TEM image. From these images, it is clear that those atoms are well dispersed, and there are no aggregates such as iron oxides.

Uniform distribution of Fe atoms was also supported by the comparison of bulk and surface compositions. In the case of LVPO-Fe-A, Fe/V ratio was 0.084 in the bulk and 0.18 in the surface. If $Fe(acac)_3$ complex was only deposited on surface, the surface Fe/V ratio observed by XPS spectra was above 1.05, taking the escape depth of 3 nm and average particle size of 75 nm observed from SEM images into account. However, the Fe/V ratio in surface was six times smaller (0.18) than the estimated value. This fact indicates that $Fe(acac)_3$ is mainly inserted into the interlayer of LVPO. On the other samples, the surface Fe/V ratio was 4–11 times higher than that in bulk, suggesting Fe-complex is partly concentrated or aggregated in surface.

Fig. 4 shows FT/IR spectra of the parent LVPO and LVPO-Fe-A. LVPO shows the band at 695, 740, 975, 1045, 1085, 1160, 1185, 1395, 1456 and 1500 cm^{-1}. These bands can be tentatively assigned to ν(P–O–C) for 1160 cm^{-1}, ν(V=O) for 975 cm^{-1}, $\nu(PO_3)$ or Ph–O stretch for 1045, 1085, 1185 cm^{-1}, deformation mode of OH of benzyl alcohol for 1395, 1456 and 1500 cm^{-1}, respectively [30–32]. After the insertion of $Fe(acac)_3$, a small bands appeared at 1283, 1368 and 1526 cm^{-1}, while the bands due to VPO layer (ν(V=O), $\nu(PO_3)$, ν(P–O–C)) were hardly affected. Spectrum c more clearly shows the difference in the spectra a and b. The bands at 936, 1283, 1368, 1526 and 1570 cm^{-1} were observed in the spectrum c which was very close to the spectrum of $Fe(acac)_3$. These bands were attributed to ν(C–C) + ν(C–O) for 936, 1283, 1526, and 1570 cm^{-1} and $\delta_s(CH_3)$ for 1368 cm^{-1}, respectively [33]. The presence of these bands attributable to $Fe(acac)_3$ suggests that the structure of $Fe(acac)_3$ is not significantly changed in the interlayer of LVPO.

From the chemical analysis shown in Table 1, P/V ratio of all the samples is around unity, and the samples are basically composed of ideal composition of V–P sheet. From the C/V ratio, 1.2 times of benzyl alcohol relative to vanadium or phosphorous are in the internal layer. It is already clarified

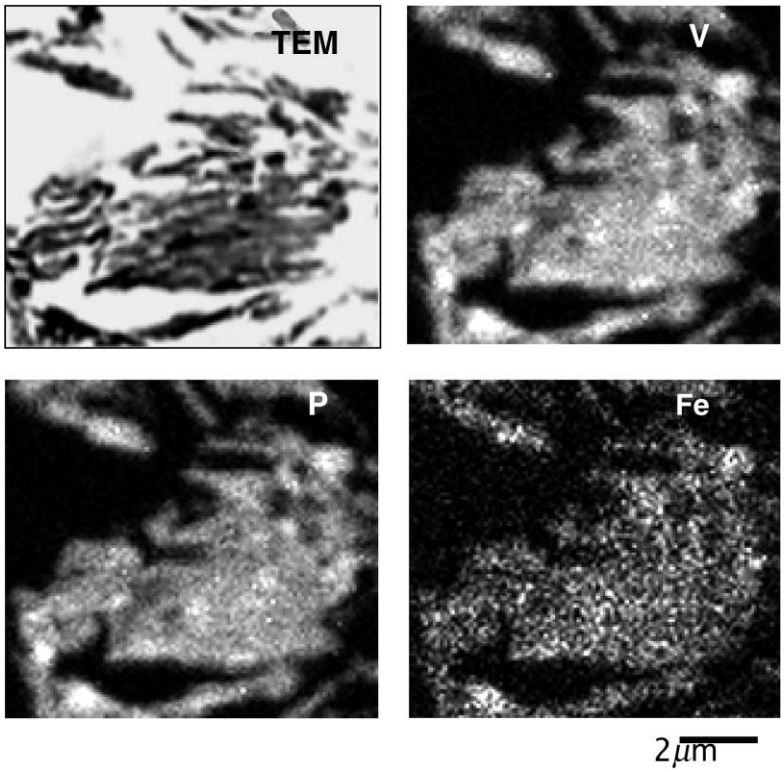

Fig. 3. TEM image of LVPO-Fe-A and EDS images of V, P and Fe.

that around a half of alcohol is settled in the layer by ester bond, and other by hydrogen bonded [28]. The TGA data of this LVPO material showed that the ratio in weak and strong bonded alcohol is around 2:1. According to these characters, the rational formula of the original LVPO-compound is $VO((C_7H_7OH)_{0.72}/H_{0.28})PO_4{\cdot}0.50C_7H_7OH$. On the other hand, the rational formula of LVPO-Fe-A is $VO((C_7H_7OH)_{0.45}/H_{0.55})PO_4{\cdot}0.18C_7H_7OH{\cdot}0.08Fe(acac)_3$. After the insertion of $Fe(acac)_3$, the number of benzyl alcohol reduced into a half. The fact indicates that $Fe(acac)_3$ was replaced with the internal alcohol. The elimination of alcohol also can be rationalized by the decrease in the interlayer distance observed in XRD patters.

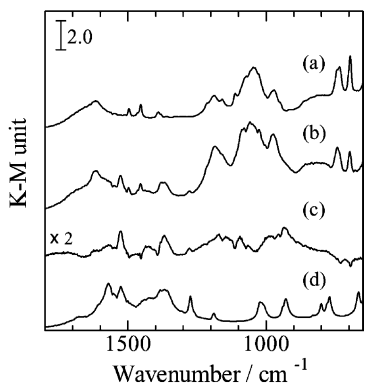

Fig. 4. FT/IR spectra of: (a) parent LVPO, (b) LVPO-Fe-A, (c) (LVPO-Fe-A)/LVPO and (d) $Fe(acac)_3$.

4. Conclusion

In the present paper, a novel approach for the preparation of well-defined promoted VPO catalysts was demonstrated. It was found that the heating of LVPO and $Fe(acac)_3$ in toluene results in the insertion of $Fe(acac)_3$ into the interlayer. Based on the results of various characterizations, the insertion of $Fe(acac)_3$

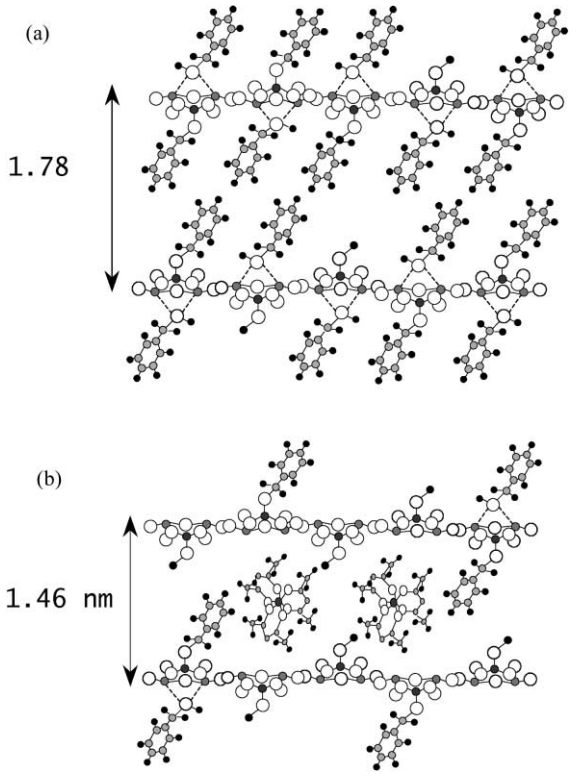

Fig. 5. Schematic model of LVPO before (a) and after (b) insertion of $Fe(acac)_3$.

into LVPO can be depicted as shown in Fig. 5, i.e., (1) internal benzyl alcohol was removed by the heating in toluene with $Fe(acac)_3$, (2) $Fe(acac)_3$ was replaced with benzyl alcohol, and (3) decrease in the internal distance occurred due to the elimination of benzyl alcohol. Further investigation on the structure of calcined VPO catalyst and catalytic profiles will be reported elsewhere.

Acknowledgements

This work was partly supported by the New Energy and Industrial Technology Development Organization (NEDO).

References

[1] B.K. Hodnett, Catal. Rev. Eng. 17 (1985) 373.
[2] E. Bordes, Catal. Today 1 (1987) 499.
[3] G. Centi, F. Trifiro, J.R. Ebner, V.M. Franchetti, Chem. Rev. 88 (1988) 55.
[4] G.J. Hutchings, Appl. Catal. 72 (1991) 1.
[5] F. Cavani, F. Trifiro, Chemtech 24 (1994) 18.
[6] F. Cavani, F. Trifiro, Catalysis, Vol. 11, Royal Society of Chemistry, Cambridge, 1994, p. 246.
[7] B.K. Hodnett, Heterogeneous Catalytic Oxidation, Wiley, New York, 2001, p. 132 (Chapter 5).
[8] V.A. Zazhigalov, J. Haber, J. Stoch, I.V. Bacherikova, G.A. Komashko, A.I. Pyatnitskaya, Appl. Catal. A 134 (1996) 225.
[9] Y. Takita, K. Tanaka, S. Ichimaru, Y. Mizuhara, Y. Abe, Y. Ishihara, Appl. Catal. A 103 (1993) 281.
[10] H.S. Horowitz, C.M. Blackstone, A.W. Sleight, G. Teufer, Appl. Catal. 38 (1988) 193.
[11] G. Busca, F. Cavani, G. Centi, F. Trifiro, J. Catal. 99 (1986) 400.
[12] M.L. Granados, J.C. Conesa, M.F. Garcia, J. Catal. 141 (1993) 671.
[13] D. Ye, A. Satsuma, A. Hattori, T. Hattori, Y. Murakami, Catal. Today 16 (1993) 113.
[14] A. Satsuma, Y. Tanaka, T. Hattori, Y. Murakami, Appl. Surf. Sci. 121–122 (1996) 496.
[15] A. Datta, R.Y. Kelar, Chem. Commun. (1996) 89.
[16] K. Beneke, G. Lagaly, Inorg. Chem. 22 (1983) 1503.
[17] G. Huan, A.J. Jacobson, J.W. Johnson, D.P. Goshorn, Chem. Mater. 4 (1992) 661.
[18] G. Huan, J.W. Johnson, J.F. Brody, D.P. Goshorn, A.J. Jacobson, Mater. Chem. Phys. 35 (1993) 199.
[19] V.V. Guliants, J.B. Benzinger, S. Sundaresan, Chem. Mater. 6 (1994) 353.
[20] V.V. Guliants, J.B. Benzinger, S. Sundaresan, Chem. Mater. 7 (1995) 1493.
[21] J.B. Benzinger, V. Guliants, S. Sundaresan, Catal. Today 33 (1997) 49.
[22] T. Doi, T. Miyake, Chem. Commun. (1996) 1635.
[23] E.M. Sabbar, M.E. de Roy, A. Ennaqadi, C. Gueho, J.P. Besse, Chem. Mater. 10 (1998) 3856.
[24] T. Nakato, Y. Furumi, T. Okuhara, Chem. Lett. (1998) 611.
[25] T. Nakato, Y. Furumi, N. Terao, T. Okuhara, J. Mater. Chem. 10 (2000) 737.
[26] J.W. Johnson, A.J. Jacobson, W.M. Butler, S.E. Rosenthatl, J.F. Brody, J.T. Lewandowski, J. Am. Chem. Soc. 111 (1989) 381.
[27] H.S. Horowitz, WO Patent 98/15353 (1998).
[28] Y. Kamiya, E. Nishikawa, Japan Kokai 11-319860 (1999).
[29] Y. Kamiya, E. Nishikawa, A. Satsuma, N. Mizuno, T. Okuhara, Sekiyu Gakkaishi 44 (2001) 265.
[30] C.J. Pouchert, The Aldrich Library of Infrared Spectra, 2nd Edition, Aldrich Chemical Company, Milwaukee, 1975.
[31] L.J. Bellamy, The Infra-red Spectra of Complex Molecules, Chapman & Hall, London, 1975, p. 353.
[32] G. Busca, F. Cavani, G. Centi, F. Trifiro, J. Catal. 99 (1986) 400.
[33] K. Nakamoto, Infrared and Raman Spectra of Inorganic and Coordination Compounds, 4th Edition, Wiley/Interscience, New York, 1986, p. 260.